THE JOURNAL OF PHYSICAL CHEMISTRY Letters

Letter

pubs.acs.org/JPCL

K-Shell Excitation and Ionization of a Gas-Phase Protein: Interplay between Electronic Structure and Protein Folding

Aleksandar R. Milosavljević,*[,†,#] Christophe Nicolas,[‡] Miloš Lj. Ranković,[†] Francis Canon,[§] Catalin Miron,[‡,∥] and Alexandre Giuliani[‡,⊥]

[†]Institute of Physics Belgrade, University of Belgrade, Pregrevica 118, 11080 Belgrade, Serbia

[‡]SOLEIL, l'Orme des Merisiers, St. Aubin, BP48, 91192 Gif sur Yvette Cedex, France

[§]INRA, UMR1324 Centre des Sciences du Goût et de l'Alimentation, F-21000 Dijon, France

[∥]Extreme Light Infrastructure - Nuclear Physics (ELI-NP), "Horia Hulubei" National Institute for Physics and Nuclear Engineering, 30 Reactorului Street, RO-077125 Măgurele, Jud. Ilfov, Romania

[⊥]INRA, UAR1008, CEPIA, Rue de la Géraudière, BP 71627, 44316 Nantes, France

Supporting Information

ABSTRACT: Understanding the correlation between proteins' tertiary and electronic structures is a great challenge, which could possibly lead to a more efficient prediction of protein functions in living organisms. Here, we report an experimental study of the interplay between electronic and tertiary protein structure, by probing resonant core excitation and ionization over a number of charge-state selected precursors of electrically charged proteins. The dependence of the core ionization energies on the protein charge state shows that the ionization of a protonated protein is strongly correlated to its tertiary structure, which influences its effective Coulomb field. On the other hand, the electronic core-to-valence shell transition energies are not markedly affected by the unfolding of the protein, from compact to totally elongated structures, suggesting that frontier protein orbitals remain strongly localized. Nevertheless, the unfolding of a protein seems to influence the cross section ratio between different resonant electronic transitions.

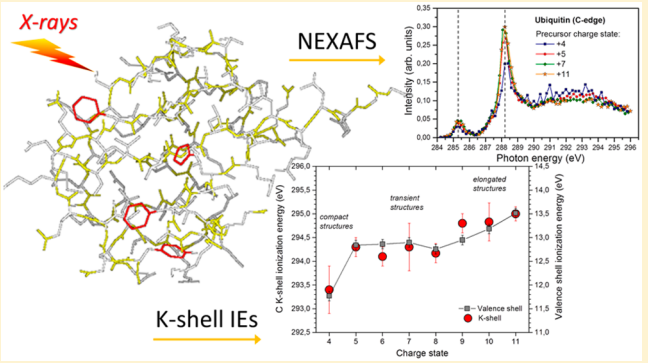

Proteins are essential for living organisms, as they accomplish numerous vital biological functions. Constituted by different polypeptide chains, proteins have in common that their functions are closely related to their three-dimensional molecular structures.[1] Therefore, long-standing research, stimulated at the same time by outstanding technological development, has been devoted to determine the average structure of a protein.[2] However, both the structural and the dynamical properties of proteins should be considered to rationalize their behavior and accurately predict their biological function.[3] The electronic structure of a protein is fundamentally correlated with its atomistic representation. Therefore, it appears important to gain a deeper understanding of the interplay between the protein electronic structure and its folding, as it could help develop methods to predict protein activity.[4,5] In order to achieve this goal, we propose an experimental approach to probe, by near edge X-ray absorption fine structure (NEXAFS) action spectroscopy,[6] the electronic structure of isolated protein ions, with some control on their three-dimensional structure provided by their level of protonation.[7] For this we use the high sensitivity and selectivity of the tandem mass spectrometry (MS^2) with the high brightness of a third-generation tunable soft X-ray synchrotron radiation source.

NEXAFS has already been established as a very sensitive method to probe the electronic structure of a wide range of samples, including biologically relevant molecules and biopolymers.[8] In recent years, proteins have come into the focus of NEXAFS, and several studies have been reported on the potential of the method to investigate protein electronic properties and even to elucidate (at least tentatively) their primary structure in combination with modeled spectra.[9,10] In NEXAFS studies of biomolecules, the X-ray absorption efficiency is probed by scanning the photon energy throughout the K-shell absorption edges. Therefore, the NEXAFS spectral features correspond to resonant excitation of a core electron to unoccupied molecular orbitals. Nevertheless, all mentioned studies with proteins were performed on thin organic films, thereby preventing control of the target's charge state and

Received: June 17, 2015
Accepted: July 28, 2015
Published: July 28, 2015

DOI: 10.1021/acs.jpclett.5b01288
J. Phys. Chem. Lett. 2015, 6, 3132−3138

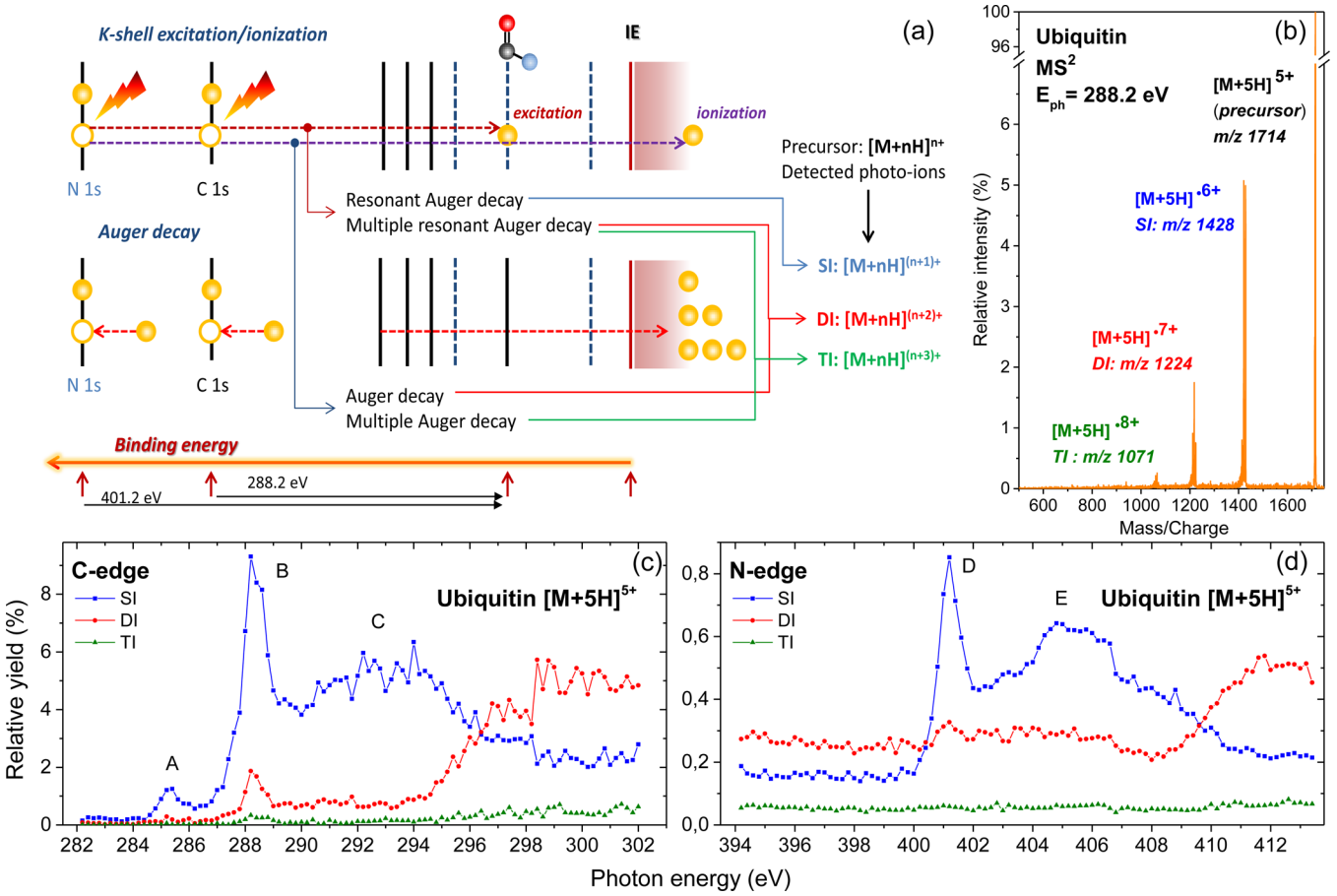

Figure 1. (a) Schematic representation of the X-ray K-shell excitation/ionization of a protein, followed by Auger decay and production of ionized cations, which are detected in the experiment. (b) Tandem ESI/photoionization mass spectrum of 5+ (m/z 1714) ion of ubiquitin protein, obtained after 500 ms of irradiation at a photon energies of 288.2 eV. (c,d) Single (SI, $[M+5H]^{6+}$, 6+ charge state, m/z 1427−1429), double (DI, $[M+5H]^{7+}$, 7+ charge state, m/z 1223−1225), and triple (TI, $[M+5H]^{8+}$, 8+ charge state, m/z 1071−1073) C and N K- edge photoionization yields of the 5+ charge state precursor $[M+5H]^{5+}$ of equine ubiquitin protein.

structure. To overcome these limitations, gas-phase study of proteins should be performed instead.

In the past two decades, mass spectrometry appeared as a very efficient tool to study the structure of proteins from their primary structure[11] up to the structure of their supramolecular edifices.[12] Recently, the introduction of the vacuum-ultraviolet (VUV) activation MS^2 has allowed determination of the binding site of a ligand on an intrinsically disordered protein, whereas classical techniques failed.[13] Among the different applications of this technique, one of the most exciting possibilities offered by such *in vacuo* spectroscopy of biological macromolecules is the investigation of their fundamental physicochemical properties.

As a proof of principle for our proposed method, we produced desolvated ubiquitin protein, in gas-phase, in different charge states ranging from +4 to +11, by means of electrospray ionization. Subsequent isolation of a selected cation, with a specific charge state, in an ion trap mass spectrometer allows us to manipulate, at least partly, its tertiary structure from a compact to an elongated geometry.[7,14] After activation of the ionic precursor by soft X-ray synchrotron radiation, a mass analysis of the produced ions is achieved (MS^2). Finally, from the recorded MS^2, a relative yield of the ionization products can be determined as a function of the photon energy, thus enabling construction of the NEXAFS action spectra (X-ray ion yields) for a desired charge-state precursor (see details below). The relationship between protein structure and charge states is now established.[15] Particularly, the case of ubiquitin has been extensively studied by ion mobility.[16] It appears that the most important structural transitions occur for states at the boundary of the elongated region. It is important to note that, in our experiments, the ion storage times are long enough to ensure that the sample has already reached equilibrium. Indeed, it requires several tenths of milliseconds from the ionization to the storage of the target ion, which is much longer than the folding dynamics of ubiquitin.[17]

In our previous work in the VUV domain, we have found a strong correlation between the folding of a gas-phase protein and its valence-shell ionization energy (IE).[7] We have also reported that an electrostatic model could be used to relate the valence-shell IE of an isolated-charge protein to its charge state and the effective radius.[7] An interesting question logically arises: Is a similar correlation seen for K-shell IEs? If the measured K-shell IEs shift in the same way, it would suggest that the unfolding of a protein changes the screening Coulomb field that affects only the ionized electron; that is, the measured correlation is a final state effect that generally relates protein's tertiary structure with its ability to be ionized by any means. Along this line, the gas-phase action NEXAFS spectroscopy can be also used to probe the protein's structure. In this letter, we demonstrate a strong correlation between K-shell and valence-shell IE dependence on the protein's charge state, suggesting

DOI: 10.1021/acs.jpclett.5b01288
J. Phys. Chem. Lett. 2015, 6, 3132−3138

that the electrostatic model reported in Giuliani et al.[7] also holds for inner-shell ionization. Moreover, unlike in the valence-shell ionization studies where only the IE can be measured, the analysis of the pre-edge features in soft X-ray absorption spectroscopy could be an additional guide to understand the interplay between electronic and tertiary protein structure.

The ionization of the photoexcited precursor at photon energies below the inner-shell ionization energy (IE) is the consequence of resonant Auger decay,[6,18] which can be briefly summarized as follows (see Figure 1a): The core (1s) electron resonantly absorbs the photon and is promoted to an unoccupied, bound molecular orbital, forming a highly excited electronic state, which decays in the femtosecond time range.[19] A valence electron fills the core vacancy, and the target relaxes by the ejection of an electron. Depending on whether the initially excited electron participates in the decay process, the process may be qualified as a participator (usually much less efficient[18]) or as a spectator, respectively. Also, it is generally energetically possible that more than one valence electron is ejected, leading to multiple resonant Auger decay.[20,21] Therefore, the processes resulting from K-shell photoexcitation of the isolated n-time multiply charged protein precursor in the present experiment can be represented by the following formula:

$$[\mathrm{M} + n\mathrm{H}]^{n+} + h\nu \rightarrow ([\mathrm{M} + n\mathrm{H}]^{n+})^{*} \rightarrow [\mathrm{M} + n\mathrm{H}]^{(n+k)+\bullet} + k\mathrm{e}^{-} \quad (1)$$

(k = 1,2,...)

In the case where the photon energy is larger than the K-shell IE, the core 1s electron is ejected into the ionization continuum, forming a core vacancy that initiates the normal Auger decay resulting in at least doubly ionized precursor:

$$[\mathrm{M} + n\mathrm{H}]^{n+} + h\nu \rightarrow ([\mathrm{M} + n\mathrm{H}]^{(n+1)+})^{*} + \mathrm{e}^{-} \rightarrow [\mathrm{M} + n\mathrm{H}]^{(n+1+k)+\bullet} + (k+1)\mathrm{e}^{-} \quad (2)$$

(k = 1,2,...)

In both cases 1 and 2, the formed radical cation can undergo further fragmentation. However, as reported previously for cytochrome c,[6] the susceptibility of gas-phase proteins to soft X-ray-induced fragmentation appears to be drastically different than it is for their amino acid building blocks, and peptides.[22] Indeed, as seen in Figure 1b for an example of the 5+ charge state precursor of ubiquitin $[\mathrm{M+5H}]^{5+}$, the ionization process, accompanied by low-mass neutral losses, represents the dominant relaxation channel upon resonant (C 1s → π^{*}_{amide}) X-ray absorption by ubiquitin. In this respect, fragmentation to small ionic fragments below the presented cutoff of about m/z 500 is negligible. The neutral losses from the ionized species produce fragments at masses close to the precursor, which appear just next to the main single ionization (SI), double ionization (DI), etc. peaks toward lower m/z, clearly resolved in the present work. Based on this fact, the present communication is focused on the ionization process as a way to probe the protein electronic structure. The signal between SI, DI, etc. processes is due to the weak fragmentation channels, but discussing these processes would be out of scope of the present Letter.

The partial ion-yield X-ray absorption spectra have been obtained from the mass spectra recorded as a function of the photon energy, after normalizing the integrated intensity of the SI, DI, and triple ionization (TI) peaks to both the total ion current and the photon flux. As explained above (see eq 1 and Figure 1a), the SI is exclusively triggered by resonant 1s excitation to unoccupied molecular orbitals (and neglecting the valence-shell ionization in this photon energy range). Therefore, the measured SI partial ion-yield X-ray absorption spectra in the present experiment represent the action NEXAFS spectra. Indeed, as also reported in our previous work,[6] the SI curve exhibits a rich spectroscopic structure allowing one to clearly resolve features that match perfectly with previously reported results from NEXAFS spectroscopy of thin protein films.[9,10] For example, electronic transitions from C 1s to molecular orbitals corresponding to $\pi^{*}_{\mathrm{C=C}}$ (aromatic) at 285.3 eV and π^{*}_{amide} (peptide bond) at 288.2 eV, as well as from N 1s to π^{*}_{amide} at 401.2 eV (bands A, B and D, respectively, in Figure 1c,d). Note that the spectra in Figure 1c are not background subtracted; therefore the direct valence-shell photoionization remains low and will thus be neglected in the following discussion, as it is known that its cross section (CS) is monotonously decreasing with photon energy.

Figure 1c,d also presents DI partial ion-yield X-ray absorption spectra (red circles). In contrast to the SI ion-yields discussed just above (blue squares), the DI curves clearly show an onset at about 294 and 408 eV, for C and N K-edge, respectively. The onsets correspond to the opening of the direct ionization channel (see Figure 1a) above the K-shell IEs. Note that the double ionization of the precursor below the C K-shell IE is dominantly produced by multiple *resonant* Auger decay (Figure 1a), triggered by the resonant 1s excitation. Therefore, the shape of the relative $[\mathrm{M} + n\mathrm{H}]^{(n+2)+}$ ion yield curve (DI) below the onset should closely reproduce the one of the relative $[\mathrm{M}+n\mathrm{H}]^{(n+1)+}$ ion yield curve (SI), which is indeed shown in Figure 2 for the case of 5+ charge state precursor.

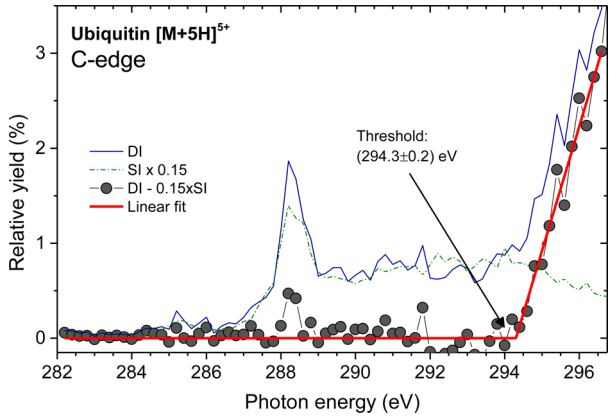

Figure 2. Normalized single (SI, $[\mathrm{M+5H}]^{6+}$, m/z 1427−1429) and double (DI, $[\mathrm{M+5H}]^{7+}$, m/z 1223−1225) C K-edge photoionization yields of the 5+ charge state precursor $[\mathrm{M+5H}]^{5+}$ of ubiquitin protein. Circles represent a difference DI − 0.15 × SI, resulting in normal Auger decay contribution of DI yields fitted to a linear threshold model (line).

Having this in mind, the subtraction of the normalized SI from the DI ion-yields should leave only a threshold curve that shows the contribution from the direct K-shell ionization (which is possible only above the IE). Figure 2 presents such a threshold curve for the case of 5+ charge state ubiquitin, together with a linear model fit that determines IE(5+) at 294.3 ± 0.2 eV (the error bars reflect the uncertainty due to both the fit and the selected fitting range). It is interesting to note that normalized SI and DI ion-yields, in fact, are different around the peak B, suggesting that the branching ratio might depend on the K-shell

DOI: 10.1021/acs.jpclett.5b01288
J. Phys. Chem. Lett. 2015, 6, 3132−3138

excitation energy (note that DI can include both double Auger ionization and Auger cascade processes). Still, this relatively small effect does not influence our adopted fitting procedure to determine IEs.

In order to determine the charge-state dependence of the C K-shell IE of ubiquitin, the C K-edge ion yields (as shown in Figure 1c) were measured for a number of charge states, in the range from 4+ to 11+ and the IEs were extracted following the procedure described above (see Figure 2). The obtained C K-shell IEs are plotted against the protein charge state in Figure 3,

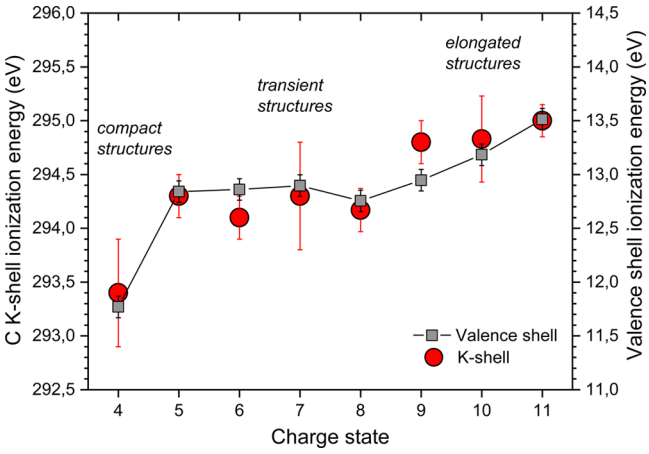

Figure 3. K-shell (circles) and valence-shell (squares)[7] ionization energies of protonated ubiquitin precursor as a function of the charge state.

together with the valence-shell IEs of ubiquitin reported recently.[7] Both curves show that an increase of the charge state of a folded protein (compact structures) would increase the IE, but as soon as the protein starts to unfold at higher protonation levels (transient structures), the effective IE remains more or less constant until the protein is totally unfolded[14] (elongated structures). Our results show that near K-edge X-ray spectroscopy has the ability to probe the tertiary structure of a protein *in vacuo*, simply by measuring the core IEs.

The C K-edge photoionization yields of ubiquitin for different precursor charge states in the overall range from +4 to +11 are compared in Figure 4a (see Supporting Information for all measured charge states). It is important to note that all curves in each panel in Figure 4a have been measured sequentially in the same experiment (see Experimental Section). This procedure ensures that the energy positions of spectral features relative to each other for different charge states are not affected by the absolute calibration of the energy scale (see Experimental section). Furthermore, the extracted spectra presented in Figure 4 are normalized to the same area (after subtraction of the background obtained as an average signal below 284 eV) in order to avoid a possible influence of different experimental conditions, particularly the target density in the trap. Indeed, according to the Thomas−Reiche−Kuhn sum rules, the area below the NEXAFS spectrum should be conserved along the charge states series.

The present measurements clearly show that the energies of the C 1s → $\pi^*_{C=C}$ (aromatics, 285.3 eV) and C 1s → π^*_{amide} (peptide bond, 288.2 eV) transitions are practically not affected by the increase of the precursor protonation from +4 to +11, at least within the limit of the present experimental uncertainty of about 0.1 eV. Supporting Figure 1 also shows that both the

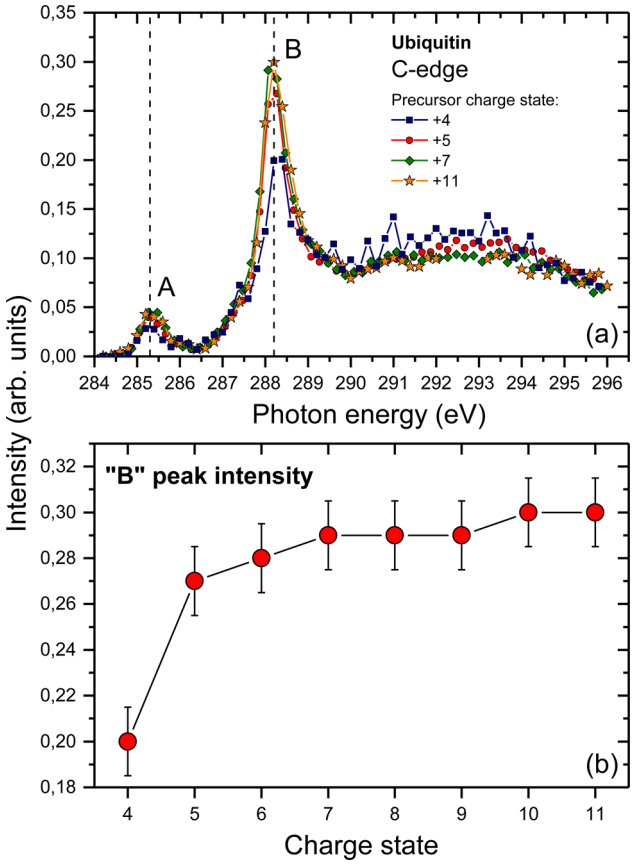

Figure 4. (a) Single C K-edge photoionization yields of the ubiquitin cation for different charge states. Dashed vertical lines mark the maximum of the A (1s → $\pi^*_{C=C\ [aromatic]}$) and B (1s → π^*_{amide} [peptide bond]) bands. (b) The intensity at the maximum of the B peak as a function of the precursor charge state.

shape and the width of the dominant band are not affected by the protonation. The same conclusions stand for the N 1s → π^*_{amide} transition, as well, although less charge states have been probed in the case of N K-edge (see Supporting Figure S2). On the other hand, the relative intensity of the dominant C 1s → π^*_{amide} resonant transition (peak B in Figure 4a) markedly depends on the protonation level as shown in Figure 4b.

Our present finding, that the resonant excitation energies are not markedly affected by the protonation (Figure 4a), may be seen as a surprise. The protonation/deprotonation of amino acids affects the charge distribution in the vicinity of their functional groups; therefore it should have a strong influence on the energetics and electronic structure of biomolecules, indeed reported previously for smaller biomolecules.[23] On the other hand, the X-ray absorption spectroscopy (XAS) does not provide information on the absolute energies of the states involved in the absorption process.[24] Therefore, the measured core excitation energies may not apparently depend on the protonation if both the core and the unoccupied valence states are similarly affected. Brown et al.[24] have recently shown this effect for protonated formic acid by combining XAS and X-ray photon spectroscopy (XPS) in a liquid microjet study. However, it is important to point out that in the present case the target biopolymer is significantly larger and is not solvated. Indeed, ubiquitin is a 76-residue protein[4] (see Supporting Information, Figure S3), so in the whole range explored, from +4 to +11 charge, one can estimate that only about 5% to 15%,

DOI: 10.1021/acs.jpclett.5b01288
J. Phys. Chem. Lett. 2015, 6, 3132−3138

respectively, of all possible local core−electron transitions to π^*_{amide} are affected by the additional charge on the functional group. Therefore, even in the case of large energy shifts, the overall contribution to the measured signal may be intrinsically hidden by the signal associated with the rest of the protein.

Although the protonation itself should not affect significantly the core excitations in the present case of a large protein complex, it should also be considered that the level of protonation defines at the same time the protein's three-dimensional structure in the gas phase.[14,16] Therefore, we simultaneously probe the influence of protein folding on core−electron excitation. In this respect, two different effects can be studied according to the results presented in Figure 4 (and the Supporting Information): (a) the K-shell excitation energies—according to the position of the bands (thus the energy of the unoccupied molecular orbitals) and (b) the relative intensity of different types of transitions (e.g., excitation to π^* or σ^* orbitals). Considering the former case (a), the folding/unfolding of the protein apparently does not affect significantly the core excitation energies to unoccupied frontier molecular orbitals. Starting from the fact that core excitation is of a very local character,[8,25] the present experimental results suggest that the unoccupied frontier protein orbitals are practically unaffected by the change of the tertiary protein's structure, even in the whole range from compact to totally unfolded and elongated structures. This result is in agreement with the prediction of previously reported complex quantum mechanical calculations for ubiquitin[4] and enzymes[5] that frontier orbitals of a protein are very localized and not affected by its dynamics. It should be noted that the measured action NEXAFS spectra do not exclude a possibility that the protein unfolding affects both the core and the unoccupied molecular orbitals, thus not significantly affecting the resonant transitions[24] (note that photoelectron spectroscopy cannot be performed in the present experiment because electrons cannot be extracted from the radiofrequency ion trap to be analyzed). Indeed, the protonation clearly produces a shift of the K-shell ionization energies. Nevertheless, there is a very good correlation between the valence and the K-shell IEs (Figure 3), suggesting that both effects represent a final state effect, which is intrinsically related to the spatial rearrangement of the charged protein. The latter affects the effective Coulomb field that influences only the ionized electron, as shown in our previous work.

On the other hand, the relative intensity of the bands corresponding to C K-shell excitations to the π^* state, as seen in Figure 4b, appears lower for lower charge states and increases with the charge state, as the protein unfolds. Interestingly enough, this increase is most pronounced in the transition from compact to unfolded structures. And it should be noted that a similar dependence has been also found for the aromatic peak A. Therefore, the tertiary structure of the protein seems to affect the relative intensity of the core-to-valence π^* transitions, the latter being less pronounced in a folded protein. Previously, Zubavichus et al.[10] investigated the formation of a macromolecule that gave rise to a 20−25% attenuation of the π^* resonances in the spectra, which they tentatively interpreted as a manifestation of conformational flexibility. The authors suggested that the molecular mass and structural flexibility of biological macromolecules could influence the NEXAFS spectra, but further research was lacking to reach solid conclusions. Indeed, the present experimental results suggest that the folding of the ubiquitin protein may induce a noticeable suppression of the π^* resonances (about 10%) in its C K-edge ion yield spectra. Following previous studies,[26] this effect can be tentatively explained by a geometrical rearrangement of C atoms with respect to each other.

In conclusion, the present experimental results provide a very first demonstration of the interplay between electronic and tertiary protein structure, by probing resonant core excitation and ionization over a number of charge-state selected precursors. The dependence of core ionization energies on the protein charge states was found to be in strong correlation with valence-shell ionization, showing that, generally, the ionization of a protonated protein is strongly correlated to its tertiary structure that influences its effective Coulomb field. On the other hand, the unfolding of the protein, from compact to totally elongated structures, practically does not influence the resonant transition energies. This experimental result is in favor of recent theoretical predictions that frontier protein orbitals remain strongly localized in a protein[45]. Nevertheless, the unfolding of a protein seems to influence the intensity ratio of different core-to-valence resonant transitions.

Finally, an interesting perspective deserves to be mentioned: the high efficiency of the X-ray-induced resonant ionization, as experimentally shown in the present measurements, clearly confirms the possibility to raise-up the production of low-energy, secondary electrons in a protein sample by orders of magnitude, by simply tuning the photon energy near the C K-edge. As pointed out in a recent theoretical study,[18] this can be of particular importance in radiation damage-related research, since the low-energy secondary electrons that interact with neighboring molecules may be a very effective source of bond breaking.[27]

EXPERIMENTAL SECTION

SR/MS^2 Spectroscopy. A commercial linear quadrupole ion trap mass spectrometer was coupled to the soft X-ray beamline PLEIADES at the synchrotron radiation facility SOLEIL (France), as described previously.[6] The photon irradiation time of 500 ms was controlled by a mechanical shutter activated by a signal sent from the spectrometer through a pulse generator that ensures a short delay of ion recording in order to reduce background contributions. The ion injection time was set to 100 ms. The X-ray beam was introduced from the back side of the trap connected to the beamline via a dedicated differential pumping stage. The electrosprayed ions were injected from the front side into the trap. The tandem mass spectra were recorded as a function of the photon energy scanned in small steps. The photon energy calibration was performed in parallel for each measurement by using an online low-pressure ion yield setup installed upstream of the mass spectrometer. The relative ion yields were extracted from the mass spectra and normalized to the total ion current and to the photon flux. For the presented action NEXAFS spectroscopy, the mass resolution has been reduced to about 1500−2000 to achieve higher signal/noise ratio, but was still more than sufficient to clearly resolve SI and DI peaks. We had a very good reproducibility of the spectra over several days of data acquisition.

The Samples. Ubiquitin protein (from Sigma-Aldrich) has been placed in water/acetonitrile solution (70:30) at 10 μM. The photon energy calibration was performed with molecular CO_2 and N_2 gas from Air Liquide, with a stated purity of 99.998% and 99.9999%, respectively.

PLEIADES Beamline. A permanent magnet APPLE II type undulator, with a period of 80 mm, was used as synchrotron

DOI: 10.1021/acs.jpclett.5b01288
J. Phys. Chem. Lett. 2015, 6, 3132−3138

radiation source. The linear polarization of the light was kept perpendicular to the plane of the electrons' orbit in the storage ring. A high-flux, 600 l/mm grating was used to monochromatize the synchrotron radiation produced by the undulator for the different K-edge regions. The exit slit of the modified Pertersen plane grating monochromator was set to reach an average resolution of 320 meV at the C-edge and 300 meV at the N-edge. The average photon fluxes at the C-edge and at the N-edge were 1.3×10^9 photon/s and 2.4×10^{10} photon/s, respectively. These fluxes take into account the carbon contamination of some of the beamline optics, and also the reduction of the incident flux by the absorption due to a pressure of 5×10^{-7} mbar CO_2 or N_2 gas present in the chamber used for calibration purposes during the measurements. The calibration gas was introduced in the calibration chamber by an effusive jet crossing at right angle the SR beam. The ions created in the interaction region are extracted by a continuous electric field detected and counted at each step of a photon energy scan. The detector consists of two polarizable grids, which attract the cations, a multichannel plates chevron stack, and a 50 Ω-adapted full-metal anode. The photon energy was calibrated according to the $Ar(2p3/2^{-1}\ 4s)$ and N 1s → π* in N_2 transitions.[19] The absolute accuracy of the energy calibration was estimated to be 50 meV for both C and N edges.

■ ASSOCIATED CONTENT

Supporting Information

The Supporting Information is available free of charge on the ACS Publications website at DOI: 10.1021/acs.jpclett.5b01288.

Additional action NEXAFS spectra for C and N K-edges, as well as adopted structure of ubiquitin protein (PDF).

■ AUTHOR INFORMATION

Corresponding Author

*E-mail: vraz@ipb.ac.rs.

Present Address

#A.R.M.: Radiation Laboratory, University of Notre Dame, Notre Dame, Indiana 46556, USA.

Notes

The authors declare no competing financial interest.

■ ACKNOWLEDGMENTS

This work was supported by the Agence Nationale de la Recherche, France, under Project ANR-08-BLAN-0065. A.R.M. and M.Lj.R. acknowledge support by the Ministry of Education, Science and Technical Development of Republic of Serbia (Projects No. 171020). A.R.M. and C.M. acknowledge support from COST action "XUV/X-ray light and fast ions for ultrafast chemistry − XLIC". The SOLEIL synchrotron radiation facility is acknowledged for providing beamtime under Project 20130382.

■ REFERENCES

(1) Rossmann, M. G.; Argos, P. Protein Folding. *Annu. Rev. Biochem.* **1981**, *50*, 497−532.

(2) Jones, N. Crystallography: Atomic Secrets. *Nature* **2014**, *505*, 602−603.

(3) Lindorff-Larsen, K.; Best, R. B.; Depristo, M. A.; Dobson, C. M.; Vendruscolo, M. Simultaneous Determination of Protein Structure and Dynamics. *Nature* **2005**, *433*, 128−132.

(4) Pichierri, F. Insights into the Interplay between Electronic Structure and Protein Dynamics: The Case of Ubiquitin. *Chem. Phys. Lett.* **2005**, *410*, 462−466.

(5) Fukushima, K.; Wada, M.; Sakurai, M. An Insight into the General Relationship between the Three Dimensional Structures of Enzymes and Their Electronic Wave Functions: Implication for the Prediction of Functional Sites of Enzymes. *Proteins: Struct., Funct., Genet.* **2008**, *71*, 1940−1954.

(6) Milosavljevic, A. R.; Canon, F.; Nicolas, C.; Miron, C.; Nahon, L.; Giuliani, A. Gas-Phase Protein Inner-Shell Spectroscopy by Coupling an Ion Trap with a Soft X-Ray Beamline. *J. Phys. Chem. Lett.* **2012**, *3*, 1191−1196.

(7) Giuliani, A.; Milosavljević, A. R.; Hinsen, K.; Canon, F.; Nicolas, C.; Réfrégiers, M.; Nahon, L. Structure and Charge-State Dependence of the Gas-Phase Ionization Energy of Proteins. *Angew. Chem., Int. Ed.* **2012**, *51*, 9552−9556.

(8) Hähner, G. Near Edge X-Ray Absorption Fine Structure Spectroscopy as a Tool to Probe Electronic and Structural Properties of Thin Organic Films and Liquids. *Chem. Soc. Rev.* **2006**, *35*, 1244−1255.

(9) Stewart-Ornstein, J.; Hitchcock, A. P.; Hernández Cruz, D.; Henklein, P.; Overhage, J.; Hilpert, K.; Hale, J. D.; Hancock, R. E. W. Using Intrinsic X-Ray Absorption Spectral Differences to Identify and Map Peptides and Proteins. *J. Phys. Chem. B* **2007**, *111*, 7691−7699.

(10) Zubavichus, Y.; Shaporenko, A.; Grunze, M.; Zharnikov, M. Is X-Ray Absorption Spectroscopy Sensitive to the Amino Acid Composition of Functional Proteins? *J. Phys. Chem. B* **2008**, *112*, 4478−4480.

(11) Aebersold, R.; Mann, M. Mass Spectrometry-Based Proteomics. *Nature* **2003**, *422*, 198−207.

(12) Van Duijn, E.; Bakkes, P. J.; Heeren, R. M. A; van den Heuvel, R. H. H.; van Heerikhuizen, H.; van der Vies, S. M.; Heck, A. J. R. Monitoring Macromolecular Complexes Involved in the Chaperonin-Assisted Protein Folding Cycle by Mass Spectrometry. *Nat. Methods* **2005**, *2*, 371−376.

(13) Canon, F.; Milosavljević, A. R.; van der Rest, G.; Réfrégiers, M.; Nahon, L.; Sarni-Manchado, P.; Cheynier, V.; Giuliani, A. Photodissociation and Dissociative Photoionization Mass Spectrometry of Proteins and Noncovalent Protein-Ligand Complexes. *Angew. Chem., Int. Ed.* **2013**, *52*, 8377−8381.

(14) Shelimov, K. B.; Clemmer, D. E.; Hudgins, R. R.; Jarrold, M. F. Protein Structure in Vacuo: Gas-Phase Conformations of BPTI and Cytochrome c. *J. Am. Chem. Soc.* **1997**, *119*, 2240−2248.

(15) Hall, Z.; Robinson, C. V. Do Charge State Signatures Guarantee Protein Conformations? *J. Am. Soc. Mass Spectrom.* **2012**, *23*, 1161−1168.

(16) Myung, S.; Badman, E. R.; Lee, Y. J.; Clemmer, D. E. Structural Transitions of Electrosprayed Ubiquitin Ions Stored in an Ion Trap over ∼ 10 Ms to 30 S. *J. Phys. Chem. A* **2002**, *106*, 9976−9982.

(17) Chung, H. S.; Ganim, Z.; Jones, K. C.; Tokmakoff, A. Transient 2D IR Spectroscopy of Ubiquitin Unfolding Dynamics. *Proc. Natl. Acad. Sci. U. S. A.* **2007**, *104*, 14237−14242.

(18) Gokhberg, K.; Kolorenč, P.; Kuleff, A. I.; Cederbaum, L. S. Site- and Energy-Selective Slow-Electron Production through Intermolecular Coulombic Decay. *Nature* **2014**, *505*, 661−663.

(19) Nicolas, C.; Miron, C. Lifetime Broadening of Core-Excited and -Ionized States. *J. Electron Spectrosc. Relat. Phenom.* **2012**, *185*, 267−272.

(20) Hitchcock, A. P.; Lablanquie, P.; Morin, P.; Lizon A Lugrin, E.; Simon, M.; Thiry, P.; Nenner, I. Ionic Fragmentation of K-Shell Excited and Ionized CO. *Phys. Rev. A: At., Mol., Opt. Phys.* **1988**, *37*, 2448.

(21) Journel, L.; Guillemin, R.; Haouas, a.; Lablanquie, P.; Penent, F.; Palaudoux, J.; Andric, L.; Simon, M.; Céolin, D.; Kaneyasu, T.; et al. Resonant Double Auger Decay in Carbon K-Shell Excitation of CO. *Phys. Rev. A: At., Mol., Opt. Phys.* **2008**, *77*, 042710.

(22) González-Magaña, O.; Reitsma, G.; Tiemens, M.; Boschman, L.; Hoekstra, R.; Schlathölter, T. Near-Edge X-Ray Absorption Mass

DOI: 10.1021/acs.jpclett.5b01288
J. Phys. Chem. Lett. 2015, 6, 3132−3138

Spectrometry of a Gas-Phase Peptide. *J. Phys. Chem. A* **2012**, *116*, 10745−10751.
(23) Ottosson, N.; Børve, K. J.; Spångberg, D.; Bergersen, H.; Sæthre, L. J.; Faubel, M.; Pokapanich, W.; Öhrwall, G.; Björneholm, O.; Winter, B. On the Origins of Core-Electron Chemical Shifts of Small Biomolecules in Aqueous Solution: Insights from Photoemission and Ab Initio Calculations of Glycine(aq). *J. Am. Chem. Soc.* **2011**, *133*, 3120−3130.
(24) Brown, M. A.; Vila, F.; Sterrer, M.; Thürmer, S.; Winter, B.; Ammann, M.; Rehr, J. J.; Van Bokhoven, J. a. Electronic Structures of Formic Acid (HCOOH) and Formate (HCOO-) in Aqueous Solutions. *J. Phys. Chem. Lett.* **2012**, *3*, 1754−1759.
(25) Miron, C.; Morin, P. High-Resolution Inner-Shell Coincidence Spectroscopy. *Nucl. Instrum. Methods Phys. Res., Sect. A* **2009**, *601*, 66−77.
(26) Zubavichus, Y.; Shaporenko, A.; Grunze, M.; Zharnikov, M. NEXAFS Spectroscopy of Homopolypeptides at All Relevant Absorption Edges: Polyisoleucine, Polytyrosine, and Polyhistidine. *J. Phys. Chem. B* **2007**, *111*, 9803−9807.
(27) Boudaïffa, B.; Cloutier, P.; Hunting, D.; Huels, M. A.; Sanche, L. Resonant Formation of DNA Strand Breaks by Low-Energy (3 to 20 eV) Electrons. *Science (Washington, DC, U. S.)* **2000**, *287*, 1658−1660.

DOI: 10.1021/acs.jpclett.5b01288
J. Phys. Chem. Lett. 2015, 6, 3132−3138